BMC Musculoskeletal Disorders

RESEARCH

Open Access

Muscle loading and endochondral ossification are involved in the regeneration of a fibrocartilaginous enthesis during tendon to bone healing in rabbits

Xiaoke Shang[1,2,3], Can Chen[2], Jiefu Zhou[3,4], Yang Yang[5*] and Jin Qu[3,4,6*]

Abstract

Purpose The purposes of the present study are to investigate the effects of reduced muscle loading by prolonged immobilization on the regeneration of fibrocartilaginous enthesis through endochondral ossification in rabbits.

Methods Forty-eight rabbits underwent standard partial patellectomy were randomly divided into the control group and the prolonged immobilization (PIM) group. The immobilized cast was only maintained for the first 4 weeks in the control group, while for the first 12 weeks or until euthanization in the PIM group. The Patella-patella tendon complexes were harvested for Micro-CT and histology at week 6, 12 and 18.

Results There was significantly lower bone volume in the PIM group than the control group at week 12, but not at week 6 and 18. At week 6, new bone was formed at the osteotomy site of the residual patella through endochondral ossification. At week 12, the chondrocytes in the tendon to bone interface were ordered and arranged in longitudinal rows separated by collagen fibres in the control group. While there were no visible fibers running continuously from tendon into bone in the PIM group. At week 18, a nearly normal fibrocartilaginous enthesis were regenerated in the control group. A similar fibrocartilaginous enthesis were also formed at the tendon to bone interface in the PIM group, but the four zones were not as distinct as that in the control group.

Conclusion Muscle loading and endochondral ossification are involved in the regeneration of a fibrocartilaginous enthesis during tendon to bone healing in this partial patellectomy model.

Keywords Muscle loading, Endochondral ossification, Tendon to bone healing, Fibrocartilaginous enthesis, Partial patellectomy

*Correspondence:
Yang Yang
yangyang86@csu.edu.cn
Jin Qu
qu.jin@csu.edu.cn
[1]Department of Orthopedic Surgery, People's Hospital of Ningxia Hui Autonomous Region, Yinchuan, China
[2]Department of Orthopaedics, Xiangya Hospital, Central South University, Changsha, China
[3]Key Laboratory of Organ Injury, Aging and Regenerative Medicine of Hunan Province, Xiangya Hospital, Central South University, Changsha, China
[4]Department of Sports Medicine, Xiangya Hospital, Central South University, Changsha, China
[5]Department of Cardiovascular Medicine, The Second Xiangya Hospital, Central South University, Changsha, China
[6]National Clinical Research Center for Geriatric Disorders, Xiangya Hospital, Central South University, Changsha, China

Introduction

Entheses are sites of stress concentration at the region where tendons and ligaments attach to bone. Although there are two fundamentally different types of entheses according to the presence or absence of fibrocartilage at the attachment sites, the fibrocartilaginous entheses (also known as direct entheses) are more common [1]. The fibrocartilaginous entheses consist of four zones: fibrous tendon/ligament, unmineralized fibrocartilage, mineralized fibrocartilage and bone [2]. Unfortunately, the fibrocartilaginous entheses with four zones are hardly regenerated after repairing tendon to bone, such as rotator cuff repair and anterior cruciate ligament (ACL) reconstruction [3]. Therefore, thousands of studies have been designed to explore how to promote tendon to bone healing, especially the regeneration of the unmineralized fibrocartilage and mineralized fibrocartilage at the tendon to bone interface [4, 5], which consumes a lot of manpower and material resources.

An understanding of the natural development of the enthesis may allow scientists to develop biomimetic strategies for enhancing tendon to bone healing by regenerating nearly normal fibrocartilaginous enthesis. The fibrocartilaginous enthesis has many similarities to the structure of the growth plate that is formed during endochondral ossification of bone [6, 7]. The development of fibrocartilaginous enthesis also follows pathways similar to those seen in the development of growth plate [6]. The Indian hedgehog-parathyroid hormone-related protein (Ihh-PTHrP) signaling pathway play essential roles in endochondral ossification at the growth plate via regulating chondrocyte proliferation and differentiation, and also play critical roles in the development of a natural fibrocartilaginous enthesis [7, 8]. Based on anatomical studies, the fibrocartilage in tendons and ligaments is an adaptation to compressive stress [9]. Where tendons and ligaments are subject to compression, they are frequently fibrocartilaginous. There is also a good correlation between the distribution of fibrocartilage within entheses and the levels of compressive stress [9]. While based on animal's studies, muscle loading is necessary for the development and formation of a natural fibrocartilaginous enthesis [6, 10]. Reduced muscle loading during postnatal development impairs fibrocartilage formation at the entheses and leads to disorganized fiber distribution and inferior mechanical properties [6, 10]. It is unknown which kind of mechanical loading (muscle tensile force or compressive stress) are predominant in the fibrocartilage development of the entheses.

The partial patellectomy model in rabbits is firstly reported by Ling Qin and his colleagues [11, 12], and gradually used to study tendon to bone healing with varied strategies [13, 14]. The Patella-patella tendon (PPT) complex is an anatomical structure comprising multiple types of tissues to meet the biomechanical demands in transmitting large tensile force allowing loading direction change and to sustain enormous compressive stress for generating joint motion [15]. Thus, the partial patellectomy model could provide a unique observation of the remodeling of tendon to bone healing under different kinds of mechanical loading. Most importantly, it is different from the tendon to bone healing in rotator cuff repair and ACL reconstruction, in which fibrous healing is dominated and the fibrocartilaginous entheses with four zones are hardly regenerated [3]. While a nearly normal fibrocartilaginous enthesis with four zones could be regenerated at the tendon to bone interface in this partial patellectomy model at the late stage of healing [16, 17]. Although it is unknown how this occurred, we speculated that the tensile force of the quadriceps muscle and endochondral ossification should play an important role in the regeneration of the fibrocartilage at the tendon to bone interface in this unique model. Therefore, the purposes of the present study are to investigate the effects of reduced muscle loading force by prolonged immobilization on the regeneration of fibrocartilaginous enthesis at the tendon to bone interface through endochondral ossification using this unique animal model.

Methods

The Animal protocol has been approved by the animal research committee of our local institution. The animal studies have adhered to the ARRIVE guidelines.

Animal surgery and assignment

Forty-eight mature female New Zealand white rabbits (weight 3.5 ± 0.2 kg) underwent standard partial patellectomy in the right hind limb using a previously established protocol [18] and were randomly divided into the control group and the prolonged immobilization (PIM) group. In brief, after the rabbits were anesthetized with 3% sodium pentobarbital (1 mL/kg intravenous injection, Sigma), the right knees were shaved and approached through a lateral skin incision. Transverse osteotomy was performed between the proximal 2/3 and the distal 1/3 of the patella with a hacksaw. The distal 1/3 patella and the fibrocartilage zone at the PPT junction were removed and two evenly spaced tunnels with a diameter of 0.8 mm were drilled longitudinally through the remaining patella from the osteotomy surface. The patellar tendon was sutured back to the remaining patella via the two tunnels with an absorbable PDS II suture (No. 3 – 0; Ethicon). A figure-of-eight tension band wire (0.6 mm diameter stainless steel wire) was additionally applied around the superior pole of the patella and tibia to protect the repair suture from overstretching. The two ends of the stainless steel wire were connected by twisting. The twisted steel wire was only kept 3–4 cycles and the distal twisted steel wire

was removed. The operated knee was then immobilized at the resting position using a cast. The immobilized cast was only maintained for the first 4 weeks in the control group, while for the first 12 weeks or until euthanization in the PIM group. Tramadol (25 mg/L) was administered via the animals' drinking water for 7 days postoperatively. Free cage activity was allowed after removal of the immobilized cast. Rabbits were euthanized with an overdose of sodium pentobarbital at postoperative week 6, 12 and 18 ($N=8$ per time point in each group). The sample size was decided based on previous studies [19]. The PPT complexes were harvested and wrapped with 0.9% saline gauze and stored in plastic bags at -20 °C until further analysis.

Micro-CT scanning

The PPT complexes were fixed in 4% neutral buffered formalin and then washed with 0.9% saline to remove the residual formalin. The samples were scanned by micro-CT (μCT 100, Scanco Medical) with 30-μm voxel size. Bone was segmented from the marrow and soft tissue for subsequent analysis using a global threshold, which was set to equal 210. Values equal to or greater than the threshold were used for representing bone tissue, whereas values below the threshold represented bone marrow and soft tissue. The newly formed bone at the PPT healing interface was separated from the remaining patella by the osteotomy site. The bone volume (BV), bone volume/tissue volume (BV/TV), bone surface area/total volume (BS/TV), trabecular thickness (Tb.Th), and trabecular spacing (Tb.Sp), and degree of anisotropy (DA) were measured and evaluated.

Histological analysis

After Micro-CT scanning, the specimens were decalcified with a 1:1 mixture of 50% formic acid and 20% sodium citrate and then embedded in paraffin. 7 μm thickness sections were prepared from the mid-sagittal plane of the PPT complex with a microtome (Microm HM 325, Thermo Scientific). The slides were stained with hematoxylin and eosin (H&E), Masson-trichrome staining and Safranin O-Fast Green for descriptive analysis of the newly formed bone and tendon to bone healing interface.

Statistical analysis

All measurements were expressed as mean ± standard deviation (SD). All analyses were performed using SPSS (version 23.0 for Windows, SPSS Inc, Chicago, Illinois). One-way analysis of variance (ANOVA) was used to detect differences between the two groups. Statistical significance was set at $P<0.05$.

Results

No severe complications were observed in either group. In the control group, after the cast was removed at postoperative week 4, the rabbits began to use the operated limb to walk. The figure-of-eight fixation wires were found ruptured at postoperative week 12 and week 18 when harvesting samples, but not at week 6. In the PIM group, after the immobilized cast was removed at postoperative week 12, the rabbits began to use the operated limb to walk. The figure-of-eight fixation wires were found ruptured at postoperative week 18 when harvesting samples, but not at week 6 and week 12. The broken modes of figure-of-eight fixation wires were found around the site of twisting in two types (loosening of twisting or fracture of the steel wires). The articular cartilage surfaces appeared normal with no evidence of advanced joint degeneration.

Micro-CT analysis

In the 3D midsagittal plane, an outgrowth of newly formed bone was found at the remaining proximal patella at postoperative week 6, 12 and 18 in both groups (Fig. 1). The BV of new bone increased gradually over time in both groups. At week 6 and 18, there was no significant difference in BV between two groups (Fig. 1D). At week 12, there was significantly lower BV in the PIM group than the control group (Fig. 1D). The BV/TV did not show any statistically significant difference between the two groups at week 6, 12 and 18 (Fig. 1H) (Table 1). Three-Dimensional morphometric analysis revealed more advanced remodeling with better alignment of the bone matrix and the formation of larger marrow cavities (Table 1). The newly formed bone was gradually oriented and anisotropic along the long axis of muscle loading, which was indicated by higher DA (Table 1). The morphology of the newly formed bone in the control group was similar to that of the native patella at week 18 (Fig. 1C).

Histological analysis

At postoperative week 6, both in the control and PIM group, the trabecular bone was newly formed at the osteotomy site of the residual patella through endochondral ossification similar to that in bone fracture healing (Fig. 2). There were different types of chondrocytes, especially hypertrophic chondrocytes, appeared at the tendon to bone interface. These chondrocytes were unordered and not arranged in longitudinal rows separated by parallel collagen fibres (Fig. 2).

At postoperative week 12, in the control group, the newly formed bone was prolonged and remodeled gradually through endochondral ossification in comparison with week 6. There was early formation of new short fibers running continuously from tendon into bone.

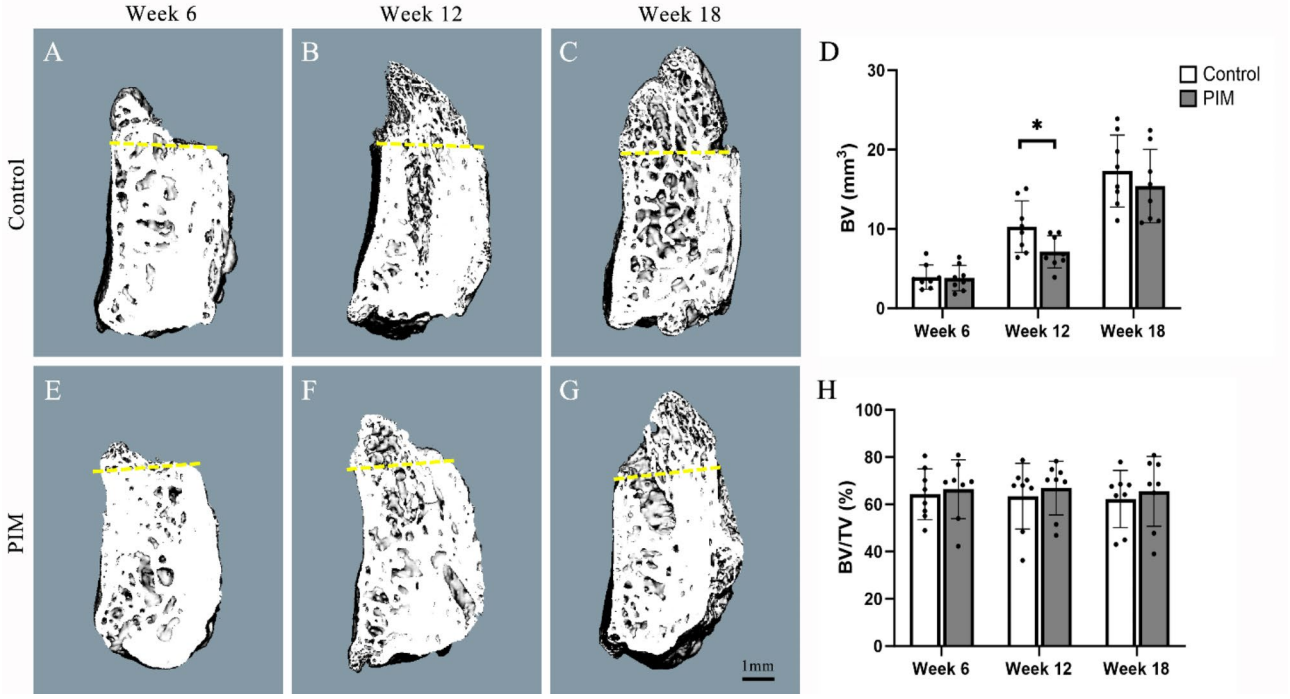

Fig. 1 Representative micro-CT images of the midsagittal plane of the Patella. **A**-**C**: Control Group; **F**-**H**: Prolonged immobilization (PIM) group. A and F: Week 6; **B** and **G**: Week 12; C and H: Week 18. The dotted line indicates the osteotomy site. **D** and **H**: Comparison of the bone volume (BV) and bone volume to total volume (BV/TV) in newly formed bone. *Significant difference between the control group and PIM group ($P < 0.05$)

Table 1 Morphometric analysis of the newly formed bone

	Week 6		Week 12		Week 18	
	Control	PIM	Control	PIM	Control	PIM
BV (mm^3)	3.94 ± 1.53	3.81 ± 1.60	10.28 ± 3.25	7.12 ± 2.04*	17.30 ± 4.54	15.41 ± 4.61
BV/TV (%)	64.30 ± 10.76	66.44 ± 12.47	63.48 ± 13.91	66.92 ± 11.35	62.25 ± 12.10	65.50 ± 14.82
BS/TV (1/mm)	11.06 ± 2.58	11.57 ± 2.35	9.15 ± 2.61	10.71 ± 1.95	6.53 ± 1.68	6.76 ± 1.66
Tb.Th (μm)	77.04 ± 9.11	75.00 ± 7.10	92.44 ± 10.58	81.73 ± 8.67*	113.70 ± 10.94	127.43 ± 17.23
Tb.Sp (μm)	42.17 ± 13.01	40.89 ± 13.95	48.54 ± 14.27	43.87 ± 12.96	68.17 ± 16.44	62.78 ± 14.04
DA [1]	1.43 ± 0.1	1.40 ± 0.11	1.58 ± 0.16	1.48 ± 0.12	1.74 ± 0.16	1.69 ± 0.18

BV: Bone volume; BV/TV: Bone volume/total volume; BS/TV: Bone surface area/total volume; Tb.Th: Trabecular thickness; Tb.Sp: Trabecular spacing; DA: Degree of anisotropy. *Statistical significance compared with the control group at the same time point: $P < 0.05$

The chondrocytes in the tendon to bone interface were ordered and arranged in longitudinal rows separated by parallel collagen fibres (Fig. 3A-D). Hyaline cartilage-like cartilaginous metaplasia was developed in the interface next to the articular cartilage of the remaining patella. While in the PIM group, the newly formed bone was slightly prolonged through endochondral ossification in comparison with week 6. There were no visible newly formed collagen fibers running continuously from tendon into bone. These chondrocytes were still unordered and not arranged in longitudinal rows separated by parallel collagen fibres (Fig. 3E-H). The cartilaginous metaplasia was also formed but less obvious in the interface next to the articular cartilage of the remaining patella.

At postoperative week 18, in the control group, a nearly normal fibrocartilaginous enthesis with four zones was regenerated at the tendon to bone interface though the remodeling was not completed. The newly formed bone was further prolonged and there was distinct formation of new collagen fibers running continuously and perpendicularly from tendon into bone. The chondrocytes in the tendon to bone interface were surrounded by the interwoven network of collagen fibres or laid in rows between parallel fibres. The chondrocytes were also ordered in the direction of tensile force, along the axis of the patella-patellar tendon complex. There was a partial mineralization front similar to the tidemark between unmineralized fibrocartilage and mineralized fibrocartilage (Fig. 4A-D). The density of chondrocytes decreased in the cartilaginous metaplasia under compression. While in the PIM group, the newly formed bone was also further prolonged and remodeled. A similar fibrocartilaginous enthesis was

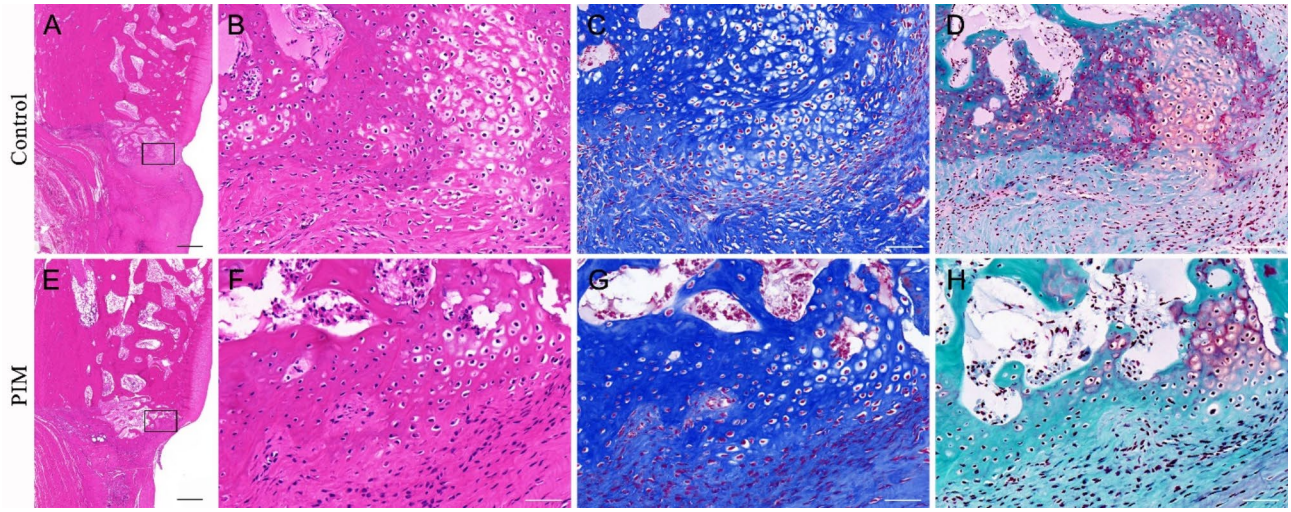

Fig. 2 Representative mid-sagittal sections of PPT complexes at week 6. **A**-**D**: Control Group; **E**-**H**: PIM group. **B**-**D**: the magnified region selected from the black rectangles in **A**; **E**-**H**: the magnified region selected from the rectangles in **E**. Black bar = 1 mm; White bar = 200 μm

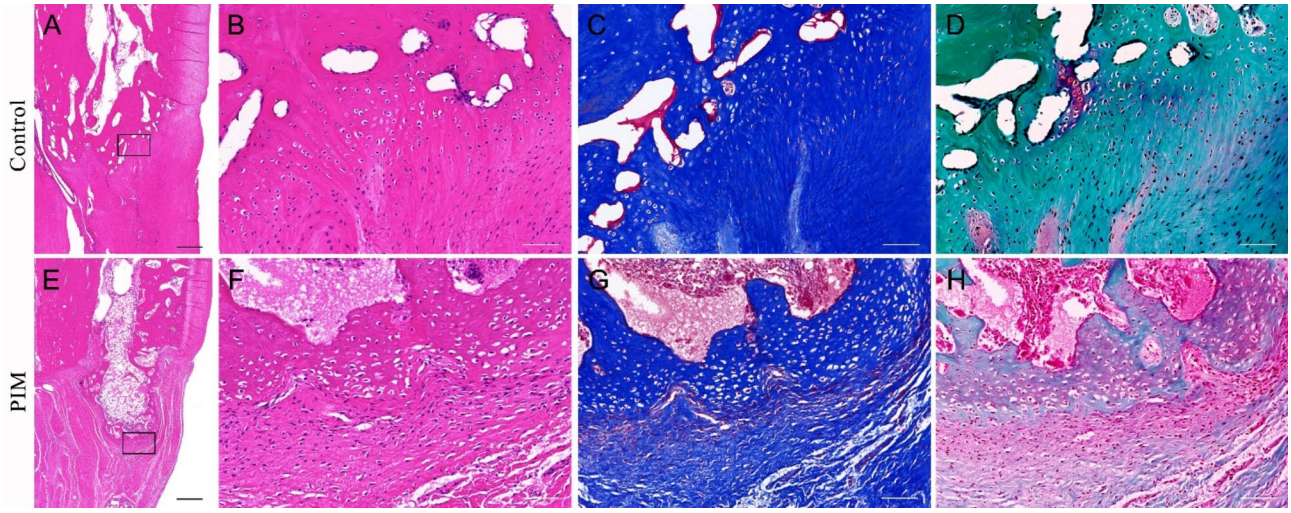

Fig. 3 Representative mid-sagittal sections of PPT complexes at week 12. **A**-**D**: Control Group; **E**-**H**: PIM group. **B**-**D**: the magnified region selected from the black rectangles in **A**; **E**-**H**: the magnified region selected from the circles in E. Black bar = 1 mm; White bar = 200 μm

also formed at the tendon to bone interface, but the four zones were not as distinct as that in the control group. The chondrocytes in the tendon to bone interface were surrounded by less organized collagen fibres. There was also a partial but inconspicuous mineralization front similar to the tidemark (Fig. 4E-H). The cartilaginous metaplasia was characterized with less cellular density and larger fibrochondrocytes. However, the healing and remodeling was still incomplete as compared to the normal entheses in both groups.

Discussion

The partial patellectomy repair model serves as a good model to evaluate the effects of tensile force and compressive stress on tendon to bone healing due to the uniqueness of the PPT complex. The current study demonstrated that reduced muscle loading force by prolonged immobilization impaired the formation of fibrocartilaginous entheses at the tendon to bone interface through endochondral ossification. The muscle force drove the fibrochondrocytes at the entheses to arrange in a columnar pattern between penetrated collagen fibers along the axis of the PPT complex. The formation of hyaline cartilage-like metaplasia next to the articular cartilage of the remaining patella should be owing to the compressive stress.

Mechanical loading plays an important role in tendon to bone healing. Both the figure-of-eight wiring and cast immobilization were used to protect the repair in this model. In the control group, after removal of the cast at postoperative week 4, the figure-of-eight fixation wires were found ruptured at week 12. The figure-of-eight

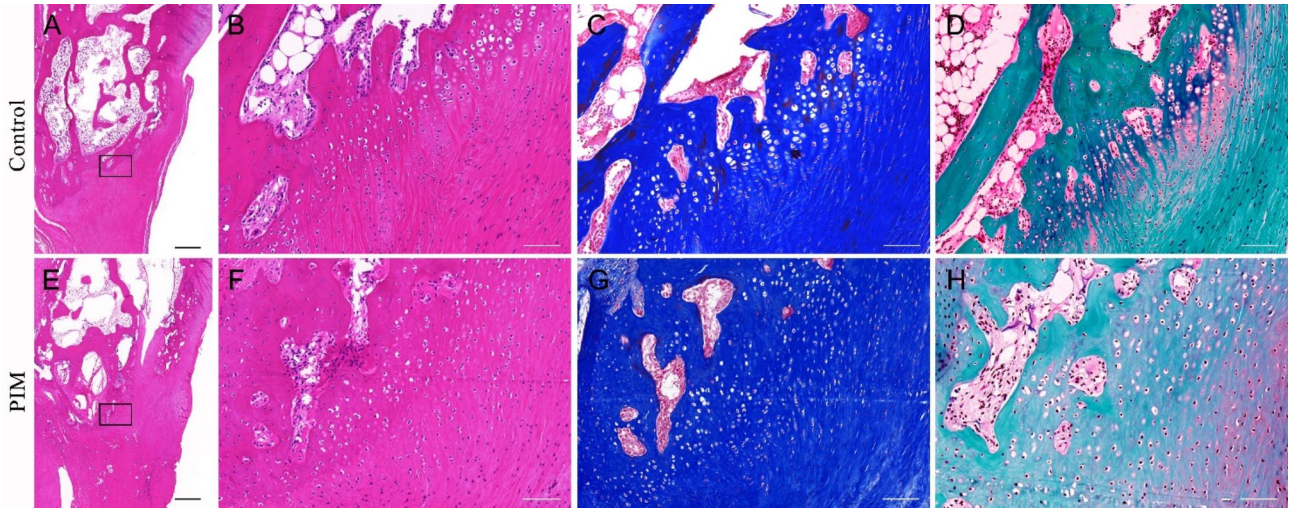

Fig. 4 Representative mid-sagittal sections of PPT complexes at week 18. **A**-**D**: Control Group; **E**-**H**: PIM group. **B**-**D**: the magnified region selected from the black rectangles in **A**; **E**-**H**: the magnified region selected from the circles in E. Black bar = 1 mm; White bar = 200 μm

fixation wires should have been broken even before week 8 according to previous related studies [20, 21]. While in the PIM group, the figure-of-eight fixation wires were found intact until the removal of the cast at week 12. There was significantly lower BV in the PIM group than the control group at week 12. Prolonged immobilization impaired and delayed the regeneration of the fibrocartilaginous entheses at the tendon to bone interface. The prolonged intact figure-of-eight fixation wires leaded by prolonged immobilization should have reduced the tensile force going through the patella-patellar complexes and thus might affect the regeneration of the fibrocartilaginous entheses.

The concept of tendon to bone healing has changed from the ossification and incorporation of the tendon into the bone [22], to ossification or formation of a fibrous sleeve of callus [23], to bone ingrowth into the tendon [24]. The mechanical strength of tendon to bone healing was positively correlated with the amount of new bone formation [21, 24]. There are two types of ossification: intramembranous and endochondral. The primary way endochondral ossification is distinguished from intramembranous ossification is the fact that cartilage is present during endochondral ossification. Fibrocartilaginous entheses are mainly developed at the epiphyses of long bones and the short bones of the tarsus or carpus [9], where bone is primarily formed by endochondral ossification. Moreover, the fibrocartilaginous enthesis has many similarities to the structure of the growth plate that is formed during endochondral ossification of bone [6]. Lu and Thomopoulos [3] summarized that the development of the fibrocartilaginous entheses was initially driven by endochondral ossification. Cartilage mineralized to form bone, and a fibrocartilaginous transition then developed at the interfaces between the bone and connective tissues. In this partial patellectomy model, the histological results indicated the fibrocartilaginous entheses with four zones regenerated at the tendon to bone interface via the cellular process of endochondral ossification. In the control group, there was also new formation of collagen fibers running continuously from tendon into bone. The chondrocytes in the tendon to bone interface were ordered and arranged in longitudinal rows separated by the interwoven network of collagen fibres or laid in rows between parallel fibres. The chondrocytes were also ordered in the direction of tensile force, along the axis of the PPT complex. While the formation of new collagen fibers was impaired and delayed by the reduced tensile loading in the PIM group. The newly formed bone through endochondral ossification and newly formed penetrated collagen fibers drove by tensile loading eventually formed the fibrocartilaginous entheses with four zones.

The natural tendon to bone healing was mostly dominated by fibrous healing in the literature. Rodeo et al. [24] studied the tendon to bone healing in an extra-articular tendon transfer model in dogs. They described a continuity between the collagen fibers and the surrounding bone with resembled Sharpey fibers. Grana et al. [25] reported a semitendinosus autograft healing in a femoral bone tunnel in a rabbit model. They also observed a fibrous enthesis with Sharpey fibers formed at the tendon to bone interface. Similarly, Goradia et al. [26] reconstructed ovine ACL with a semitendinosus free graft and reported regeneration of a fibrous enthesis characterized with Sharpey fibers. In the bone tunnel, mechanical loading occurs mainly by shear forces, which might prevent the development of a fibrocartilage zone and lead to the development of a fibrous enthesis. Different from the above, there were only very limited publications

reported a fibrocartilaginous enthesis with four zones regenerated at the tendon to bone interface during natural healing process. Weiler et al. [27] for the first time reported that a fibrocartilaginous enthesis with four zones could be regenerated during ACL reconstruction with a soft-tissue graft and an inside-out interference screw fixation. They divided the tendon to bone healing in ACL reconstruction into intra-tunnel healing and surface healing. A fibrocartilaginous enthesis was formed at the surface healing, while a fibrous healing occurred at the intra-tunnel healing. They speculated that shear forces in the tunnel might lead to the development of such an indirect insertion and allow minor longitudinal movements between the graft tissue and the surrounding bone. In contrast, at the joint surface, tensile forces acted mainly perpendicular on the tendon to bone interface and might facilitate to a regeneration of a fibrocartilaginous enthesis. Yamakado et al. [28] investigated the tendon-to-bone healing under different mechanical loading using an extra-articular model in rabbits and found that tensile force enhanced the regeneration of a fibrocartilaginous enthesis, compressive stress promoted a chondroid cell transformation, and shear force had little or no effect on regeneration of the enthesis. Wong et al. [29] evaluated the tendon healing in different regions of a bone trough using a partial patellectomy model in goats. At the base of the bone trough, a fibrocartilaginous enthesis with perpendicular bridging fibers was formed subjected to tensile force. While at the edge of the bone trough, a fibrous enthesis with oblique fibers was formed subjected to shear force. The orientation of penetrating fibers was aligned along the line of forces. In the current study, after the figure-of-eight fixation wires ruptured, patellar tendon transmitted muscle force in the direction of the longitudinal axis of the patella. The tensile forces acted mainly perpendicular on the tendon to bone interface and facilitated to the formation of penetrated collagen fibers running continuously from tendon into bone. A nearly normal fibrocartilaginous entheses with four zones were therefore regenerated at the tendon to bone interface based on the cellular process of endochondral ossification.

Mechanical loading plays a critical role in maintaining the homeostasis of native musculoskeletal tissues. A fibrocartilaginous transition zone did not develop between the supraspinatus tendon and the humeral head until postnatal time points [10]. Pauwels [30] described the morphological cell transformation into chondroid cells when the soft-tissue was exposed to compressive loads. Moreover, compressive loads change tendon into a fibrocartilaginous morphology, mostly evident where tendons wrap around bony pulleys [31]. Compression stress leads to production of aggrecan, a large proteoglycan in cartilage and thought to play a role in providing resistance to compression [32]. There is also a good correlation between the distribution of fibrocartilage within an enthesis and the levels of compressive stress [9]. In summary, fibrocartilage in tendons and ligaments is usually developed under compressive stress. While tensile loading of tendon increases its stiffness, with organization of tendon collagen fibres, and increases cell strain in the direction of loading [33]. Besides, tensile force leads to the production of proteins associated with tendon (e.g., type I collagen) [34]. In this partial patellectomy model, the presence of fibrocartilage might be viewed as an adaptation to postoperative tensile force generated to the PPT healing junction. The tensile force was almost parallel to the long axis of PPT complex and might thus explain the development of a fibrocartilage zone with chondroid cells aligning between orientated collagen fibers. In contrast, the formation of cartilaginous metaplasia next to the articular cartilage of the remaining patella should be owing to the compressive stress. Thomopoulos et al. have demonstrated that muscle loading forces were necessary for the development of a functional tendon enthesis, while unloading led to a loss of fibrocartilage transitional tissue at the tendon-to-bone attachment [10, 35, 36]. According to the findings of Schneider and Küsswetter [37], the tensile forces transmitted by the collagen fibers create compressive stress to these cells laying between the fibers. Decreased muscle loading probably led to decreased compressive stress on chondral cells laying between the collagen fibers and subsequently affected the formation of fibrocartilage at tendon to bone interface.

The present study has several limitations. Firstly, as there are several differences in knee between rabbits and humans, the findings of the study should not be simply generalized to patients associated with tendon to bone healing. Secondly, there are also several differences in tendon to bone healing among rotator cuff repair, ACL reconstruction and partial patellectomy model. Endochondral ossification and tensile loading are involved in the regeneration of a fibrocartilaginous enthesis during tendon to bone healing in the partial patellectomy model. More research is needed to clarify the role of endochondral ossification and tensile loading on tendon to bone healing in other models. Thirdly, the present study did not assess the healing quality in terms of the tensile strength of the tendon to bone healing interface. Several previous studies have evaluated the healing strength in this partial patellectomy model [20, 21]. The failure line resulting from the tensile testing mostly occurred between the newly formed bone and the residual proximal patella, not at the newly formed fibrocartilaginous enthesis between the newly formed bone and patella tendon. The purpose of the study was to explore the effects of endochondral ossification and tensile loading on the

regeneration of fibrocartilaginous enthesis in this partial patellectomy model. In addition, previous study has demonstrated that the size of the newly formed bone after partial patellectomy is positively correlated with the failure load in tensile testing [21]. It is speculated that there would be lower failure load in the PIM group in comparison with the control group. Fourthly, the figure-of-eight fixation wires were found ruptured at different time point between the PIM and control group. These suggest prolonged immobilization should have reduced the tensile force going through the patella-patellar complexes. Unfortunately, it was hard to quantitatively detect the differences of muscle loading between the two groups.

Conclusions

In summary, a reduction in muscle loading force by prolonged immobilization impaired the formation of fibrocartilaginous entheses with four zones at the tendon to bone interface. Endochondral ossification and muscle loading are involved in the regeneration of a fibrocartilaginous enthesis during tendon to bone healing in this partial patellectomy model.

Abbreviations

PIM	Prolonged immobilization
Micro-CT	Micro-computed tomography
ACL	Anterior cruciate ligament
PPT	Patella-patella tendon
BV	Bone volume
BV/TV	Bone volume/total volume
BS/TV	Bone surface area/total volume
Tb.Th	Trabecular thickness
Tb.Sp	Trabecular spacing
DA	Degree of anisotropy
3D	Three dimensional

Acknowledgements

We acknowledge the assistance of the investigators in our department.

Author contributions

XS, CC, YY and JZ contributed to the study design, the acquisition, analysis, data interpretation, and data collection. XS, YY and JQ contributed to the statistical analysis and manuscript preparation. All authors read and approved the final manuscript.

Funding

This work was supported by the grants from the Natural Science Foundation of Hunan Province (2023JJ30895), National Natural Science Foundation of China (No. 81501898) and Xiangya Hospital of Central South University. This work was also supported by the grant from the Natural Science Foundation of Ningxia Hui Autonomous Region (2020A0534).

Data availability

The data are available from the corresponding author upon reasonable request.

Declarations

Ethics approval and consent to participate

Animal experiments in this study were conducted in compliance with nationally or internationally recognized guidelines, and approved by the Laboratory Animal Committee of Xiangya Hospital of Central South University (No. 202110103).

Consent for publication

Not applicable.

Competing interests

The authors declare no competing interests.

Received: 31 July 2023 / Accepted: 7 March 2025
Published online: 19 March 2025

References

1. Benjamin M, Kumai T, Milz S, et al. The skeletal attachment of tendons–tendon entheses. Comp Biochem Physiol Mol Integr Physiol. 2002;133(4):931–45.
2. Benjamin M, Evans EJ, Copp L. The histology of tendon attachments to bone in man. J Anat. 1986;149:89–100.
3. Lu HH, Thomopoulos S. Functional attachment of soft tissues to bone: development, healing, and tissue engineering. Annu Rev Biomed Eng. 2013;15:201–26.
4. He HB, Wang T, Wang MC, et al. Tendon-to-bone healing after repairing full-thickness rotator cuff tear with a triple-loaded single-row method in young patients. BMC Musculoskelet Disord. 2021;22(1):305.
5. Huang X, Jia Q, Li H, et al. Evaluation of sparing the pronator quadratus for volar plating of distal radius fractures: a retrospective clinical study. BMC Musculoskelet Disord. 2022;23(1):625.
6. Thomopoulos S, Genin GM, Galatz LM. The development and morphogenesis of the tendon-to-bone insertion - what development can teach Us about healing. J Musculoskelet Neuronal Interact. 2010;10(1):35–45.
7. Fang F, Sup M, Luzzi A, et al. Hedgehog signaling underlying tendon and enthesis development and pathology. Matrix Biol. 2022;105:87–103.
8. Zelzer E, Blitz E, Killian ML, et al. Tendon-to-bone attachment: from development to maturity. Birth Defects Res C Embryo Today. 2014;102(1):101–12.
9. Benjamin M, Ralphs JR. Fibrocartilage in tendons and ligaments–an adaptation to compressive load. J Anat. 1998;193(Pt 4):481–94.
10. Thomopoulos S, Kim HM, Rothermich SY, et al. Decreased muscle loading delays maturation of the tendon enthesis during postnatal development. J Orthop Res. 2007;25(9):1154–63.
11. Qin L, Leung KS, Chan CW, et al. Enlargement of remaining patella after partial patellectomy in rabbits. Med Sci Sports Exerc. 1999;31(4):502–6.
12. Leung KS, Qin L, Leung MC, et al. Partial patellectomy induces a decrease in the proteoglycan content in the remaining patellar articular cartilage. An experimental study in rabbits. Clin Exp Rheumatol. 1999;17(5):597–600.
13. Li M, Chen Y, Hu J, et al. Sustained release of collagen-affinity SDF-1alpha from book-shaped acellular fibrocartilage scaffold enhanced bone-tendon healing in a rabbit model. J Orthop Res. 2021;39(6):1331–43.
14. Zheng C, Lu H, Tang Y, et al. Autologous Freeze-Dried, Platelet-Rich plasma carrying Icariin enhances Bone-Tendon healing in a rabbit model. Am J Sports Med. 2019;47(8):1964–74.
15. Flandry F, Hommel G. Normal anatomy and biomechanics of the knee. Sports Med Arthrosc Rev. 2011;19(2):82–92.
16. Lu H, Qin L, Lee K, et al. Healing compared between bone to tendon and cartilage to tendon in a partial inferior patellectomy model in rabbits. Clin J Sport Med. 2008;18(1):62–9.
17. Lu H, Qin L, Cheung W, et al. Low-intensity pulsed ultrasound accelerated bone-tendon junction healing through regulation of vascular endothelial growth factor expression and cartilage formation. Ultrasound Med Biol. 2008;34(8):1248–60.
18. Lu H, Chen C, Qu J, et al. Initiation timing of Low-Intensity pulsed ultrasound stimulation for Tendon-Bone healing in a rabbit model. Am J Sports Med. 2016;44(10):2706–15.
19. Hu J, Qu J, Xu D, et al. Combined application of low-intensity pulsed ultrasound and functional electrical stimulation accelerates bone-tendon junction healing in a rabbit model. J Orthop Res. 2014;32(2):204–9.
20. Lu H, Qin L, Fok P, et al. Low-intensity pulsed ultrasound accelerates bone-tendon junction healing: a partial patellectomy model in rabbits. Am J Sports Med. 2006;34(8):1287–96.
21. Lu H, Hu J, Qin L, et al. Area, length and mineralization content of new bone at bone-tendon junction predict its repair quality. J Orthop Res. 2011;29(5):672–7.
22. Kernwein G, Fahey J, Garrison M. The fate of tendon, fascia and elastic connective tissue transplanted into bone. Ann Surg. 1938;108(2):285–90.

23. Whiston TB, Walmsley R. Some observations on the reactions of bone and tendon after tunnelling of bone and insertion of tendon. J Bone Joint Surg Br. 1960;42–B:377–86.
24. Rodeo SA, Arnoczky SP, Torzilli PA, et al. Tendon-healing in a bone tunnel. A Biomechanical and histological study in the dog. J Bone Joint Surg Am. 1993;75(12):1795–803.
25. Grana WA, Egle DM, Mahnken R, et al. An analysis of autograft fixation after anterior cruciate ligament reconstruction in a rabbit model. Am J Sports Med. 1994;22(3):344–51.
26. Goradia VK, Rochat MC, Grana WA, et al. Tendon-to-bone healing of a semitendinosus tendon autograft used for ACL reconstruction in a sheep model. Am J Knee Surg. 2000;13(3):143–51.
27. Weiler A, Hoffmann RF, Bail HJ, et al. Tendon healing in a bone tunnel. Part II: histologic analysis after biodegradable interference fit fixation in a model of anterior cruciate ligament reconstruction in sheep. Arthroscopy. 2002;18(2):124–35.
28. Yamakado K, Kitaoka K, Yamada H, et al. The influence of mechanical stress on graft healing in a bone tunnel. Arthroscopy. 2002;18(1):82–90.
29. Wong MW, Qin L, Lee KM, et al. Healing of bone-tendon junction in a bone trough: a goat partial patellectomy model. Clin Orthop Relat Res. 2003;413:291–302.
30. Pauwels F. Eine neue theorie Über Den einfluß mechanischer Reize auf die differenzierung der stützgewebe. Z Für Anatomie Und Entwicklungsgeschichte. 1960;121(6):478–515.
31. Vogel KG, Koob TJ. Structural specialization in tendons under compression. Int Rev Cytol. 1989;115:267–93.
32. Takahashi I, Nuckolls GH, Takahashi K, et al. Compressive force promotes sox9, type II collagen and Aggrecan and inhibits IL-1beta expression resulting in chondrogenesis in mouse embryonic limb bud mesenchymal cells. J Cell Sci. 1998;111(Pt 14):2067–76.
33. Freedman BR, Rodriguez AB, Hillin CD et al. Tendon healing affects the multiscale mechanical, structural and compositional response of tendon to quasi-static tensile loading. J R Soc Interface. 2018;15(139).
34. Wang JH, Guo Q, Li B. Tendon biomechanics and mechanobiology–a minireview of basic concepts and recent advancements. J Hand Ther. 2012;25(2):133–40. quiz 141.
35. Schwartz AG, Lipner JH, Pasteris JD, et al. Muscle loading is necessary for the formation of a functional tendon enthesis. Bone. 2013;55(1):44–51.
36. Abraham AC, Fang F, Golman M, et al. The role of loading in murine models of rotator cuff disease. J Orthop Res. 2022;40(4):977–86.
37. Schneider H. Zur struktur der Sehnenansatzzonen. Z Für Anatomie Und Entwicklungsgeschichte. 1956;119(5):431–56.

Publisher's note